J. Plasma Phys. (2023), *vol*. 89, 935890603
Published by Cambridge University Press
doi:10.1017/S0022377823001319

Loss and revival of coherence in the interaction between a positron beam and a photon field

F. Castelli[1,2], S. Cialdi[1,2], G. Costantini[3,4], R. Ferragut[2,5], M. Giammarchi[2,†], G. Gittini[6], M. Leone[5], G. Maero[1,2], S. Olivares[1,2], M. Romé[1,2], A. Simonetto[6] and V. Toso[1,2]

[1]Dipartimento di Fisica, Università degli Studi di Milano, Via Celoria 16, 20133 Milano, Italy

[2]INFN, Sezione di Milano, Via Celoria 16, 20133 Milano, Italy

[3]Dipartimento di Ingegneria dell'Informazione, Università degli Studi di Brescia, Via Branze 38, 25123 Brescia, Italy

[4]INFN, Sezione di Pavia, Via Bassi 6, 27100 Pavia, Italy

[5]L-NESS and Dipartimento di Fisica, Politecnico di Milano, Via Anzani 42, 22100 Como, Italy

[6]CNR-ISTP, Via R. Cozzi 53, 20125 Milano, Italy

(Received 30 July 2023; revised 10 November 2023; accepted 17 November 2023)

We study the interaction between a positron beam in the single-particle regime in an interferometric configuration and a microwave electromagnetic field. We discuss the conditions under which quantum interference can be affected by the field and we outline its possible experimental study in the framework of QUantum interferometry and gravitation with Positrons and LASers (QUPLAS) experiment.

Key word: intense particle beams

1. Introduction

The study of open quantum systems describes the possible interactions of a system showing quantum properties with any kind of external perturbation. They can be distinguished between two major categories: a first group in which the characteristics contained in the quantum system are being irreversibly lost or degraded (Markovian systems), and a second in which information is transmitted or exchanged between the quantum system and the environment (non-Markovian systems) (Breuer *et al.* 2016).

Matter–wave experiments performed in vacuum allow the investigation of the first category, for example, by observing the loss of contrast of the interferometric pattern while degrading the vacuum level of the experimental set-up, as was demonstrated in Hornberger *et al.* (2003) and Schütz *et al.* (2015). Here, the quantum phase information is lost and the interference patterns are irreversibly washed away by a series of scatterings of the particles with the residual gas.

In the second category, we can find the quantum systems that interact coherently with other physical systems possessing well-defined phase properties, thereby making possible the exchange of the information between the two systems. They are based on the fact

† Email address for correspondence: marco.giammarchi@mi.infn.it

that the interaction is non-dissipative in its essence. Under these conditions, the change in visibility of an interferometric pattern might show the effect of 'quantum revival': an oscillatory behaviour of the visibility as the interaction parameter between the two systems monotonically increases. This is, for instance, the case when an interferometric pattern is suitably made to interfere with a laser system. Such revivals can also be found by investigating other aspects such as coherence, entanglement and quantum correlations (Maniscalco, Olivares & Paris 2007; Vasile *et al.* 2010; Benatti, Floreanini & Olivares 2012; Cialdi *et al.* 2019).

Focusing on matter–wave interference experiments in the non-Markovian case, this condition has been studied and observed in Chapman *et al.* (1995), where an atom interferometer has been subjected to the perturbation induced by single photons. Our study here differs from Chapman *et al.* (1995) in two fundamental aspects: first of all, we consider the quantum revival effect between an antiparticle (as opposed to a particle) and a coherent electromagnetic field. Secondly, we discuss an interaction case where the massive system (and not the photon) is in the single-particle mode.

In essence, we pave the way for studying the revival effect in a single-particle mode, never studied before (by using antiparticles).

The basis and inspiration for this work is the first detection of antiparticle (positron) interference in our QUPLAS (QUantum interferometry and gravitation with Positrons and LASers) experiment (Sala *et al.* 2019). This interference, obtained with a Talbot–Lau configuration (Sala *et al.* 2015; Sala, Giammarchi & Olivares 2016), has been obtained in single-particle mode, similarly to the historical experiment with electrons performed by Merli, Missiroli & Pozzi (1976).

2. The strategy

The first stage of the QUPLAS experiment featured a positron beam coupled with a Talbot–Lau interferometer and a high-resolution emulsion detector (Anzi *et al.* 2020; Ariga *et al.* 2020). In the experimental configuration, the two gratings have different periods ($d_1 = 1.2\,\mu\text{m}$ and $d_2 = 1\,\mu\text{m}$, respectively) so that the configuration acts as a magnifier of the diffraction pattern. The distance L_1 between the two gratings (see figure 1) is set to $L_1 = d_1 d_2/\lambda$ (Sala *et al.* 2019), where $\lambda = h/mv$ is the De Broglie wavelength, with m and v the positron mass and velocity, respectively, and h Planck's constant. In order to obtain the maximum contrast on the detector, this is located at a distance L_2 from the second grating given by the relation $L_2 = d_2 L_1/(d_1 - d_2)$.

The experiment is powered by a 50 mCi ^{22}Na positron source. After a few preparation steps, an almost monochromatic (energy spread of a few eV) positron beam with energies tuneable in the range 10–20 keV is obtained. At these velocities, the particles pass through the interferometer in a fraction of μs. Taking into account all the losses due to solid angle, moderation and other processes, the flux turns out to be $\simeq 10^4$ particles s^{-1}. Taking into account the paucity of this beam and the fact that the radioactive material is an incoherent fermionic source, the experiment is definitely in the single-particle regime.

The present configuration, featuring two silicon nitride material gratings, will be supplemented by a microwave cavity, located after the second grating, as shown in figure 1, providing a standing (∼10 GHz) electromagnetic field. Therefore, the positrons crossing the second grating will interact with the photons in the microwave cavity. This interaction can be described by a Hamiltonian of the form (Friedman *et al.* 1988; Henke *et al.* 2021)

$$\hat{H} \simeq \hbar g(\hat{a}^\dagger \hat{b} + \hat{a}\hat{b}^\dagger), \tag{2.1}$$

https://doi.org/10.1017/S0022377823001319 Published online by Cambridge University Press

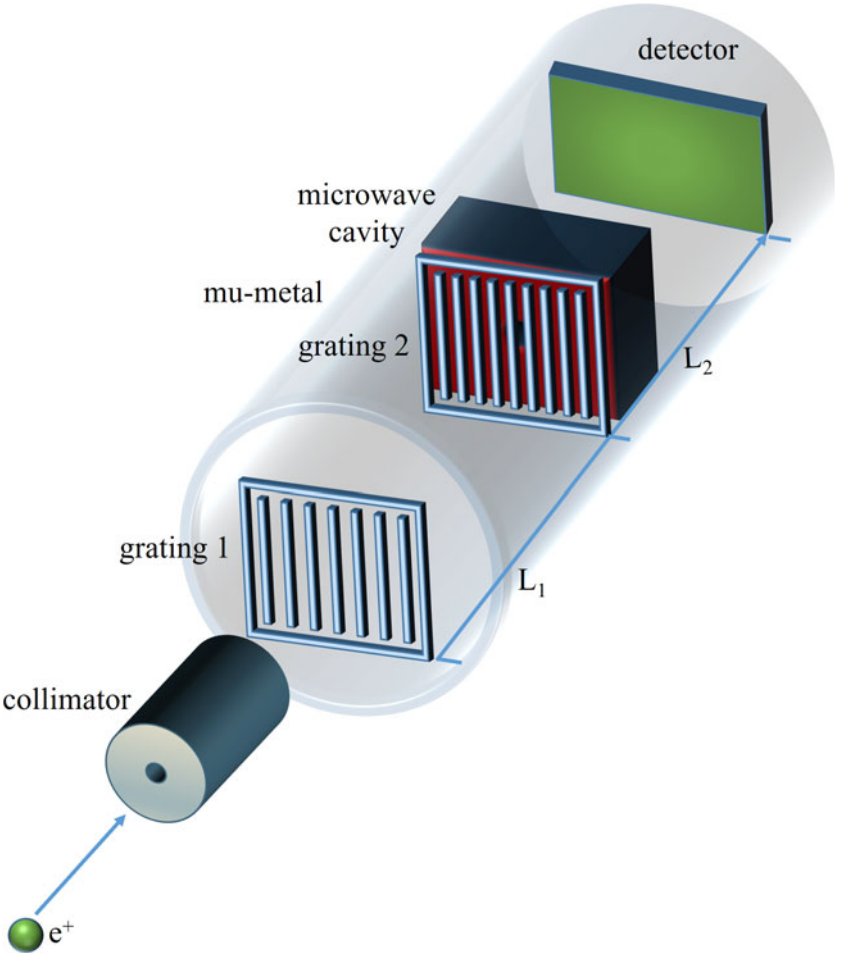

FIGURE 1. The QUPLAS configuration for this study and principle of operation. A collimated positron beam is followed by a system of gratings. The interference pattern is recorded by a high-resolution emulsion detector. The set-up is equipped with a microwave cavity to study the proposed particle–wave interaction.

where a and $a^\dagger$ are the boson field annihilation and creation operators, $[a, a^\dagger] = 1$, g is a coupling constant and b the positron-energy ladder operator, reducing its energy by the energy of one microwave photon and changing its linear momentum. This interaction produces an entanglement between positrons and photons, having the form

$$|\psi_e, \psi_\gamma\rangle \simeq \sum_n c_n |E - n\hbar\omega\rangle |n\rangle, \tag{2.2}$$

where n is the number of exchanged photons (having frequency ω) and c_n are amplitudes. Different effects are then obtained as a function of the power in the microwave cavity, which is related to the number of photons in the expansion. In the case of a small coupling constant, $|\psi_e, \psi_\gamma\rangle$ is dominated by the effect of one or two photons

$$|\psi_e, \psi_\gamma\rangle \simeq |E\rangle|0\rangle + g|E - \hbar\omega\rangle|1\rangle + g^2|E - 2\hbar\omega\rangle|2\rangle. \tag{2.3}$$

https://doi.org/10.1017/S0022377823001319 Published online by Cambridge University Press

In the presence of a macroscopic, monochromatic microwave field, namely, a coherent state of the radiation field, we can substitute for $\hat{a}$ in (2.1) the complex amplitude α of the microwave field, that reduces to a momentum-displacement operation, in analogy with the same kind of operation in quantum optics (Olivares 2021).

In principle, one should solve the Schrödinger equation with the above Hamiltonian for the proposed experimental configuration. In order to simplify the problem we have developed two complementary approaches:

(i) the two-slit model;
(ii) the Gaussian–Schell model (GSM).

In the two-slit model, the grating structure is geometrically simplified down to the simplest Young-like configuration, taken to grasp the essence of the phenomenon. The idea is to model a single positron passing through the interferometer and interacting with the microwave cavity. On the other hand, the GSM is an analytical model used for the statistical treatment of partially coherent beams. Both models will be shown to give consistent results.

3. The two-slit model

The two-slit model assumes that the essence of the phenomenon is equivalent to considering two neighbouring slits belonging to the second grating, as shown in figure 2. We assume that a non-relativistic positron is propagating along the z direction, while the grating slits are parallel to the x direction (orthogonal to the (y, z) plane shown in figure 2); under these conditions, interference will show up along the y axis. The microwave cavity is modelled as a rectangular wave guide with length w and transverse dimensions a and b. Considering only the fundamental mode TE_{10} of the wave guide, the stationary field is characterized by a longitudinal wavenumber

$$k_L = \sqrt{\left(\frac{2\pi\nu_0}{c}\right)^2 - \left(\frac{2\pi\nu_c}{c}\right)^2}, \tag{3.1}$$

where ν_0 is the frequency of the microwave field, and $\nu_c = c/2a$ the cutoff frequency of the TE_{10} mode.

The vector potential of the confined microwave field in the cavity is given by

$$A_z = \frac{E_0}{\omega}\cos\left(\frac{\pi x}{a}\right)\sin(k_L y)\cos(\omega t + \varphi), \tag{3.2}$$

where E_0 is the amplitude of the electric field, $\omega = 2\pi\nu_0$ and φ is a phase. The origin of the coordinates is placed at the centre of the opening for the passage of positrons into the microwave cavity. Assuming the diameter of this opening is much smaller than the linear dimensions of the microwave cavity and of the wavelength of the TE_{10} mode inside the cavity, the potential (3.2) can be simplified as

$$A_z \simeq \frac{E_0}{\omega} k_L y \cos(\omega t + \varphi). \tag{3.3}$$

The amplitude of the wave electric field in the wave guide can be written in terms of the time-averaged (over a wave period) peak power P by means of the relation

$$E_0 = \sqrt{\frac{4P\eta}{wa}}, \tag{3.4}$$

where $\eta = 1/\epsilon_0 c\sqrt{1 - (\nu_c/\nu_0)^2}$ is the wave impedance.

https://doi.org/10.1017/S0022377823001319 Published online by Cambridge University Press

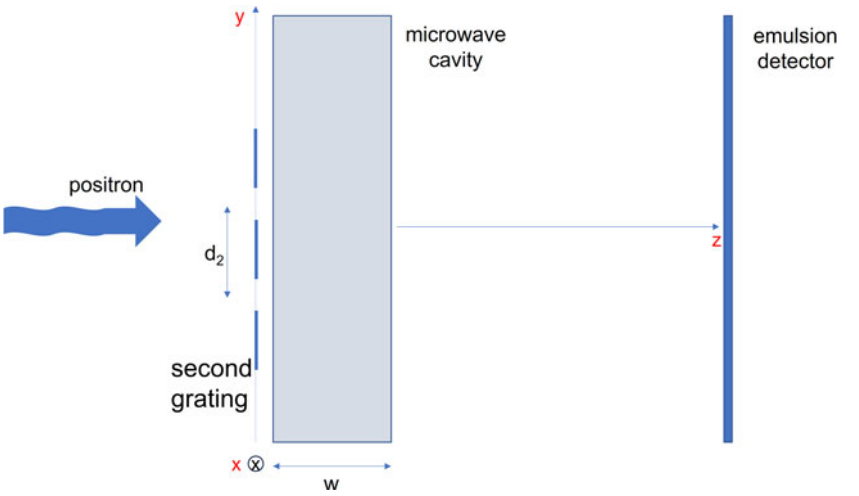

FIGURE 2. The two-slit model can be visualized as two independent sources located at the end of the second grating of QUPLAS, where a microwave cavity is positioned. The x axis is pointing into the figure, away from the reader.

Neglecting the term proportional to the square of the vector potential (low amplitude wave electric field), the Hamiltonian of the interaction between the particle and the field reads

$$H \simeq -\frac{e}{m} A_z p_z, \tag{3.5}$$

where e is the positron charge, and $p_z \simeq mv$ (neglecting the transverse velocity components of the particle).

The effect due to two neighbouring slits is summarized by an overall shift

$$\begin{aligned}\Delta\phi(P, \varphi; w, a, \omega, d_2) &= -\frac{1}{\hbar}\int_0^\tau H_2 \,\mathrm{d}t + \frac{1}{\hbar}\int_0^\tau H_1 \,\mathrm{d}t \\ &\simeq -\frac{1}{\hbar}\sqrt{P\eta\frac{w}{a}}\frac{e}{\pi v}k_L d_2 \frac{1}{\tau}\int_0^\tau \cos(\omega t + \varphi) \\ &= -\frac{1}{\hbar}\sqrt{P\eta\frac{w}{a}}\frac{e}{\pi v}k_L d_2 \frac{\sin(\omega\tau + \varphi) - \sin(\varphi)}{\omega\tau},\end{aligned} \tag{3.6}$$

where $\tau \simeq w/v$ is the crossing time of the positron in the wave field, and H_1 and H_2 denote the interaction Hamiltonian relevant to the passage of the particle through slits 1 and 2, respectively, separated by a distance d_2 (i.e. the period of the second grating).

For a uniform random distribution of the phase φ, the degree of decoherence introduced by the stationary field can be quantified by means of

$$D(P; w, a, \omega, d_2) = \frac{1}{2\pi}\int_{-\pi}^{\pi} \exp[\mathrm{i}\Delta\phi(P, \varphi; w, a, \omega, d_2)]\,\mathrm{d}\varphi. \tag{3.7}$$

The function D is real and coincides with the visibility of the interference pattern. An example of the dependence of D on microwave power is given in figure 3.

https://doi.org/10.1017/S0022377823001319 Published online by Cambridge University Press

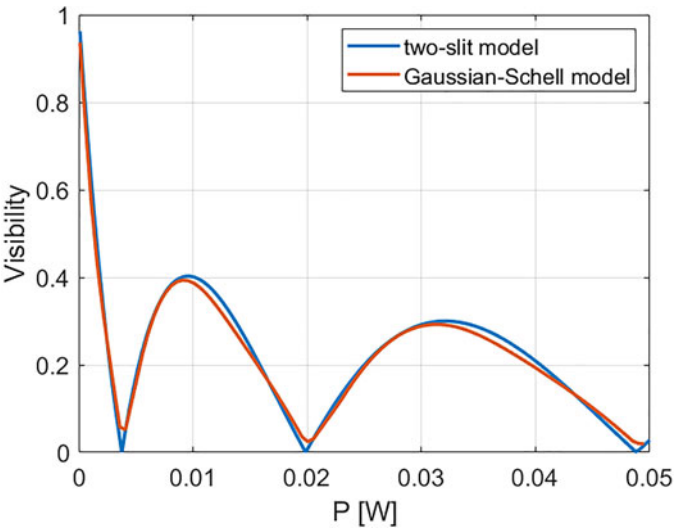

FIGURE 3. Visibility of the fringes as a function of the power of the microwave field in both the two-slit model and in the GSM model for positrons with 14 keV kinetic energy, $\nu_0 = 10$ GHz, $w = 4$ mm, $a = 21.2$ mm and $d_2 = 1\,\mu$m. The additional data used in the GSM model are $d_1 = 1.2\,\mu$m, $l_0 = 0.65$ nm, $w_0 = 2.8$ mm; the two gratings are assumed to have a transparency $f_1 = f_2 = 0.5$. The visibility is computed at the z-coordinate of the Talbot–Lau maximum.

4. The Gaussian–Schell model

The same physical problem has been addressed by means of a simulation that makes use of an analytical description of the beam, namely the GSM (McMorran & Cronin 2008).

In the GSM, the partial coherence and wavefront curvature of a beam are taken into account by using a series of parameters describing the non-ideality of both the beam and of the related grating system. This approach has a great versatility, and can describe a variety of interferometric situations in different regimes (Talbot–Lau, Fraunhofer, Mach–Zehnder...).

The model describes a partially coherent beam as a statistical distribution of Gaussian modes, characterized by its initial width, coherence length and wavefront curvature. In the simulation, we have assumed that only the transverse part contributes to the coherence length; this is due to the good monochromaticity of the QUPLAS positron beam (good longitudinal coherence) (Ariga *et al.* 2020). The ingredients used in the GSM calculation are:

(i) The mutual intensity function.
(ii) Its propagation in free space.
(iii) Its modification due to the effect of the gratings and microwave cavity.

The mutual intensity function is used in partially coherent optics, where it is considered that a beam has some momentum distribution in the direction transverse to propagation. It is defined by

$$J(\boldsymbol{x}_a, \boldsymbol{x}_b, z) = \langle \Phi^*(\boldsymbol{x}_a, z, t)\Phi(\boldsymbol{x}_b, z, t)\rangle\,, \tag{4.1}$$

where Φ is a field, $\boldsymbol{x}_a, \boldsymbol{x}_b$ are coordinates orthogonal to the z propagation direction of the beam and the angular brackets denote a time average over the statistical fluctuations of the field. This quantity describes both the spatial coherence of the beam and its intensity, as

https://doi.org/10.1017/S0022377823001319 Published online by Cambridge University Press

given by the relation

$$I(\boldsymbol{x}, z) = J(\boldsymbol{x}, \boldsymbol{x}, z). \tag{4.2}$$

Once this function is given at $z = 0$, the beam propagation in space can be described by means of the Van Cittert–Zernike theorem, that links the mutual intensity function J to the Fourier transform of the intensity of a partially incoherent source, enabling us to devise a free propagation law for J

$$J(\boldsymbol{x}, \Delta\boldsymbol{x}, z) = \frac{1}{\lambda^2 z^2} \int \mathrm{d}\Delta\boldsymbol{x}' \int \mathrm{d}\boldsymbol{x}' \exp(-(2\pi\mathrm{i}/\lambda z)(\boldsymbol{x}' \cdot \Delta\boldsymbol{x}' - \boldsymbol{x}' \cdot \Delta\boldsymbol{x} - \boldsymbol{x} \cdot \Delta\boldsymbol{x}' + \boldsymbol{x} \cdot \Delta\boldsymbol{x}))$$
$$J(\boldsymbol{x}', \Delta\boldsymbol{x}', 0), \tag{4.3}$$

where $\boldsymbol{x} = (\boldsymbol{x}_a + \boldsymbol{x}_b)/2$ and $\Delta\boldsymbol{x} = \boldsymbol{x}_b - \boldsymbol{x}_a$. This law gives the mutual intensity function J at some z, given its form at $z = 0$ for the case of free propagation.

The structure of the initial mutual intensity function is specified as

$$J(\boldsymbol{x}, \Delta\boldsymbol{x}, 0) = \exp(-\pi(\boldsymbol{x}^2/w_0^2 + \Delta\boldsymbol{x}^2/l_0^2 + 2i\boldsymbol{x} \cdot \Delta\boldsymbol{x}/\lambda r_0)), \tag{4.4}$$

where w_0 is the beam opening (width), l_0 the transverse coherence length and r_0 the radius of curvature of the wavefront. In the free propagation of the beam from $z_0 = 0$ to a generic position z, the mutual intensity function J retains the Gaussian structure, with the values of the parameters evolved as

$$w(z) = w(z_0)\sqrt{\left(1 + \frac{z}{r_0}\right)^2 + \left(\frac{\lambda z}{w_0 l_0}\right)^2}, \tag{4.5}$$

$$l(z) = l(z_0)\sqrt{\left(1 + \frac{z}{r_0}\right)^2 + \left(\frac{\lambda z}{w_0 l_0}\right)^2}, \tag{4.6}$$

$$r(z) = z\left[\frac{(1 + z/r_0)^2 + (\lambda z/w_0 l_0)^2}{(z/r_0)(1 + z/r_0) + (\lambda z/w_0 l_0)^2}\right]. \tag{4.7}$$

Concerning the initial beam parameters, they were experimentally determined by a series of runs in the standard QUPLAS configuration (without the microwave cavity) as $l_0 = 0.65$ nm and $w_0 = 2.4$ mm, neglecting the effect of the curvature radius (Sala 2018).

The action of a grating is represented by means of its transmission function μ, so that the mutual intensity function at the z-coordinate of the grating is changed as

$$J'(\boldsymbol{x}, \Delta\boldsymbol{x}, z) = \mu^*(\boldsymbol{x} - \Delta\boldsymbol{x}/2)\mu(\boldsymbol{x} + \Delta\boldsymbol{x}/2)J(\boldsymbol{x}, \Delta\boldsymbol{x}, z). \tag{4.8}$$

In order to describe material gratings realized as open slits in a substrate, μ is simply assumed in each period d as 1 in an interval of width fd (open slit), and 0 in a following interval of width $(1 - f)d$ (substrate), where f is the transparency of the grating.

After an initial phase of free propagation, the operation (4.8) is performed a first time in the position of the first grating (period and transparency d_1 and f_1, respectively), followed by a new phase of free propagation for the modified J up to the second grating. Then the mutual intensity function is changed again on the basis of (4.8) in the position of the second grating (period and transparency d_2 and f_2, respectively).

https://doi.org/10.1017/S0022377823001319 Published online by Cambridge University Press

The insertion of the microwave cavity changes the propagation after the second grating. Its effect is modelled again using (4.8) with a transmission function $\mu = \exp(\tilde{\Phi})$. Using the same approximations adopted in the two-slit model

$$\tilde{\Phi} \simeq -\frac{\mathrm{i}}{\hbar}\int_0^{\tau} H\,\mathrm{d}t \simeq 2\mathrm{i}\frac{ev}{\hbar\omega^2}\sqrt{\frac{\eta P}{wa}}k_L y\,[\sin(\omega\tau+\varphi)-\sin(\varphi)]\,. \tag{4.9}$$

The intensity at the z-coordinate of the detector is finally computed after a final phase of free propagation, and averaging over the phase φ. The resulting visibility of the interferometric pattern is shown for fixed values of the relevant parameters and compared with the result of the two-slit model in figure 3.

5. Conclusion

We have proposed and analysed the non-Markovian interaction between an antiparticle and a carefully prepared electromagnetic microwave field. The results indicate the feasibility of the experiment, currently being planned as an upgrade of the QUPLAS set-up.

This experiment can shed light on the interaction and the mutual exchange of coherence between a quantum system and an electromagnetic field, in particular, in the unexplored regime where the field interacts with a single antiparticle. We believe that such a proposal and the related experiment is an important step to improving the fundamental aspect of quantum mechanics beyond the 'matter' realm, but also to foster new experimental techniques that can be used in other anti-matter related experiments.

Acknowledgements

Editor F. Califano thanks the referees for their advice in evaluating this article.

Declaration of interests

The authors report no conflict of interest.

REFERENCES

Anzi, L., Ariga, A., Ereditato, A., Ferragut, R., Giammarchi, M., Maero, G., Pistillo, C., Romé, M., Scampoli, P. & Toso, V. 2020 Sensitivity of emulsion detectors to low energy positrons. *J. Instrum.* **15**, 03027.

Ariga, A., Cialdi, S., Costantini, G., Ereditato, A., Ferragut, R., Giammarchi, M., Leone, M., Maero, G., Miramonti, L., Pistillo, C., *et al.* 2020 The QUPLAS experimental apparatus for antimatter interferometry. *Nucl. Instrum. Meth.* A **951**, 163019.

Benatti, F., Floreanini, R. & Olivares, S. 2012 Non-divisibility and non-Markovianity in a Gaussian dissipative dynamics. *Phys. Lett.* A **376** (45), 2951–2954.

Breuer, H.-P., Laine, E.-M., Piilo, J. & Vacchini, B. 2016 Non-Markovian dynamics in open quantum systems. *Rev. Mod. Phys.* **88**, 021002.

Chapman, M.S., Hammond, T.D., Lenef, A., Schmiedmayer, J., Rubenstein, R.A., Smith, E. & Pritchard, D.E. 1995 Photon scattering from atoms in an atom interferometer: coherence lost and regained. *Phys. Rev. Lett.* **75** (21), 3783–3787.

Cialdi, S., Benedetti, C., Tamascelli, D., Olivares, S., Paris, M.G.A. & Vacchini, B. 2019 Experimental investigation of the effect of classical noise on quantum non-Markovian dynamics. *Phys. Rev.* A **100** (5), 052104.

Friedman, A., Gover, A., Kurizki, G., Ruschin, S. & Yariv, A. 1988 Spontaneous and stimulated emission from quasifree electrons. *Rev. Mod. Phys.* **60** (2), 471–535.

https://doi.org/10.1017/S0022377823001319 Published online by Cambridge University Press

HENKE, J.-W., RAJA, A.S., FEIST, A., HUANG, G., AREND, G., YANG, Y., KAPPERT, F.J., WANG, R.N., MÖLLER, M., PAN, J., *et al.* 2021 Integrated photonics enables continuous-beam electron phase modulation. *Nature* **600**, 653–658.

HORNBERGER, K., UTTENTHALER, S., BREZGER, B., HACKERMÜLLER, L., ARNDT, M. & ZEILINGER, A. 2003 Collisional decoherence observed in matter wave interferometry. *Phys. Rev. Lett*. **90** (16), 160401.

MANISCALCO, S., OLIVARES, S. & PARIS, M.G.A. 2007 Entanglement oscillations in non-Markovian quantum channels. *Phys. Rev.* A **75** (6), 062119.

MCMORRAN, B. & CRONIN, A.D. 2008 Model for partial coherence and wavefront curvature in grating interferometers. *Phys. Rev.* A **78** (1), 013601.

MERLI, P.G., MISSIROLI, G.F. & POZZI, G. 1976 On the statistical aspect of electron interference phenomena. *Am. J. Phys*. **44** (3), 306–307.

OLIVARES, S. 2021 Introduction to generation, manipulation and characterization of optical quantum states. *Phys. Lett.* A **418**, 127720.

SALA, S. 2018 QUPLAS: Towards antimatter interferometry. PhD thesis, University of Milano.

SALA, S., ARIGA, A., EREDITATO, A., FERRAGUT, R., GIAMMARCHI, M., LEONE, M., PISTILLO, C. & SCAMPOLI, P. 2019 First demonstration of antimatter interferometry. *Sci. Adv*. **5**, eaav7610.

SALA, S., CASTELLI, F., GIAMMARCHI, M., SICCARDI, S. & OLIVARES, S. 2015 Matter-wave interferometry: towards antimatter interferometers. *J. Phys.* B **48** (19), 195002.

SALA, S., GIAMMARCHI, M. & OLIVARES, S. 2016 Asymmetric Talbot-Lau interferometry for inertial sensing. *Phys. Rev.* A **94** (3), 033625.

SCHÜTZ, G., REMBOLD, A., POOCH, A., CHANG, W.T. & STIBOR, A. 2015 Electron matter wave interferences at high vacuum pressures. *Measurement* **68**, 201–204.

VASILE, R., GIORDA, P., OLIVARES, S., PARIS, M.G.A. & MANISCALCO, S. 2010 Nonclassical correlations in non-Markovian continuous-variable systems. *Phys. Rev.* A **82** (1), 012313.

https://doi.org/10.1017/S0022377823001319 Published online by Cambridge University Press